# Rydberg-atom collisions with $SF_6$ and $CCl_4$ at very high $n$

X. Ling, B. G. Lindsay, K. A. Smith, and F. B. Dunning
*Department of Space Physics and Astronomy, Rice University, Houston, Texas 77251*
*and the Rice Quantum Institute, Rice University, Houston, Texas 77251*
(Received 1 July 1991)

Rate constants for Rydberg-atom destruction through electron transfer in collisions between K($np$) Rydberg atoms and $SF_6$ and $CCl_4$ have been measured for values of principal quantum number $n$ up to $n \sim 400$ using an apparatus specifically developed for very-high-$n$ collision studies. Analysis of the data using the free-electron model provides cross sections for electron attachment to $SF_6$ and $CCl_4$ at electron energies down to $\sim 10$ $\mu$eV, which are far below those accessible using any alternate technique. The measured cross sections are inversely proportional to electron velocity and are consistent with the Wigner threshold law for $s$-wave attachment.

PACS number(s): 34.60.+z, 34.80.Gs

In recent years studies of Rydberg-atom collisions have been used to obtain information on electron attachment to electronegative molecules at subthermal electron energies [1–6]. Rydberg-atom collisions are frequently discussed using the free-electron model, in which it is assumed that the separation between the Rydberg electron and its associated ionic core is so large that both do not interact simultaneously with a target molecule [7]. At sufficiently large values of principle quantum number $n$, reactions involving attaching targets are dominated by the binary Rydberg electron-target interaction. Capture of the excited electron by the target molecule leads to Rydberg-atom destruction and the formation of a positive-negative ion pair. Previous studies, however, have been limited to Rydberg atoms with values of $n \lesssim 100$. In the present work we have extended measurements to $n \sim 400$ using an apparatus specifically developed for very-high-$n$ collision studies and have investigated Rydberg-atom destruction in collisions between K($np$) Rydberg atoms and $SF_6$ and $CCl_4$ via the electron transfer reactions

$$K(np)+SF_6 \rightarrow K^+ + SF_6^{-*} , \quad (1)$$

$$K(np)+CCl_4 \rightarrow K^+ + CCl_4^{-*} \rightarrow K^+ + CCl_3 + Cl^- . \quad (2)$$

Analysis of the data provides cross sections for electron attachment to $SF_6$ and $CCl_4$ at electron energies down to $\sim 10$ $\mu$eV, which are far below those accessible using any alternate technique, and demonstrates that, at threshold, electron capture is an $s$-wave process.

Collision studies at very high $n$ have not been undertaken previously because of the significant experimental obstacles involved. These stem from the extreme sensitivity of very-high-$n$ atoms to even very small external fields and the small oscillator strengths associated with their excitation. We have, however, overcome these difficulties using the apparatus shown in Fig. 1.

Potassium atoms contained in a tightly collimated thermal-energy ($\sim 300$ °C) beam are photoexcited to a selected $np$ state by a crossed, weakly focused laser beam. Excitation occurs at the center of an interaction region defined by three pairs of planar copper electrodes, each $\sim 10 \times 10$ cm$^2$. The use of large electrodes well separated from the excitation volume minimizes the effects of stray patch fields due to nonuniformities in the electrode surfaces. Any small residual electric fields that remain are cancelled by application of small bias potentials to the various electrodes. Magnetic fields are eliminated by use of a $\mu$-metal shield that surrounds the interaction region.

Excitation is accomplished using a frequency-doubled Coherent CR699-21 Rh6G dye laser. The output of the laser is formed into a series of pulses of $\sim 2$ $\mu$sec duration with a pulse repetition frequency of $\sim 5-10$ kHz using an acousto-optic modulator. To achieve stable excitation and reproducible laser scanning, the long-term drift in the laser output frequency is controlled using a technique that employs a scanning Fabry-Pérot étalon and stabilized He-Ne laser [8]. Rydberg-atom production is monitored by field ionization [9,10]. A voltage pulse is applied to the lower electrode and the resulting ions or electrons are detected using a particle multiplier.

The Rydberg-atom signal observed as the laser is scanned over a frequency interval corresponding to excitation of Rydberg states with $n \sim 410$ is shown in Fig. 2. The well-resolved excitation spectrum demonstrates that

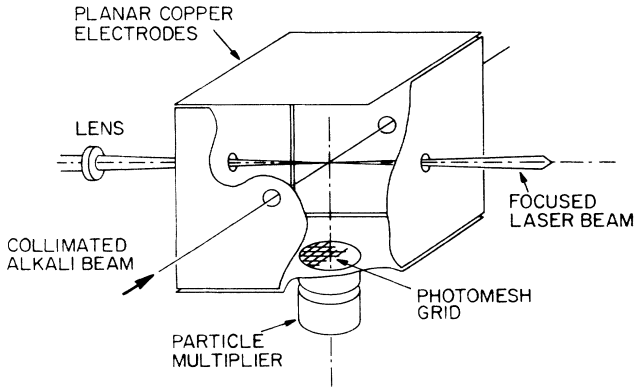


FIG. 1. Schematic diagram of the apparatus.

 

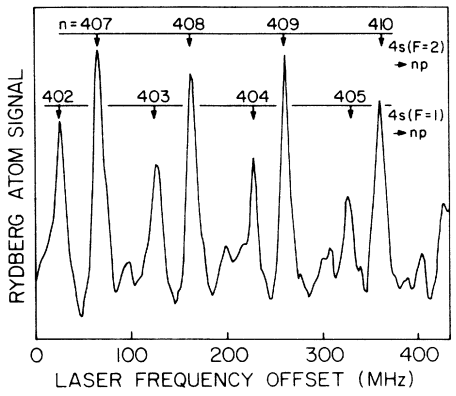


FIG. 2. Rydberg-atom production observed in the vicinity of $n \sim 410$.

stray residual fields in the excitation volume are very small. The effect of external electric fields is illustrated in Fig. 3, which shows, for several values of applied external field, the Rydberg-atom production observed as the laser is scanned over a frequency interval corresponding to excitation of states with $n \sim 270$. It is apparent that the excitation efficiency is dramatically reduced by the presence of even a very small external field. The $m_l = 0$ states are, however, more sensitive to the presence of the field.

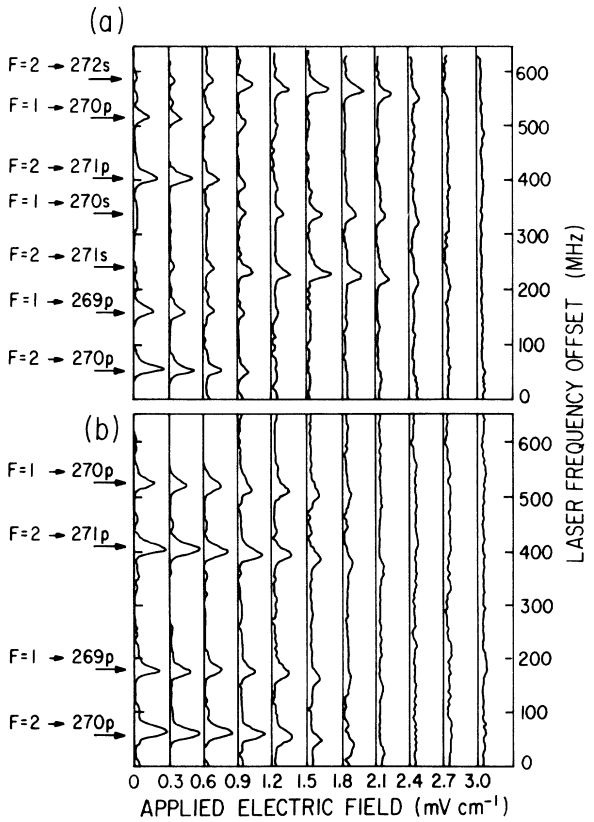


FIG. 3. The effect of applied external electric fields on the excitation of (a) $m_l = 0$ and (b) $|m_l| = 1$ states in the vicinity of $n \sim 270$.

Indeed, at "intermediate" external fields, excitation of $s$-like states made accessible through Stark mixing becomes dominant, as has been noted previously in studies at lower $n$ [11,12]. The external fields that reduce the $np$ excitation efficiency by one-half were measured as a function of $n$ and are shown in Fig. 4. For reference, the solid line indicates the electric field at which states from adjacent hydrogenic Stark manifolds first cross. It is apparent that at $n = 400$ external fields of only $\sim 100$ $\mu V\,cm^{-1}$ are sufficient to cause a significant reduction in excitation efficiency. This, coupled with the narrow width of the various excitation peaks present in Fig. 2, indicates that stray electric fields in the excitation volume are reduced to $\lesssim 50$ $\mu V\,cm^{-1}$ using the present apparatus.

For collision experiments, excitation occurs (in zero electric field) in the presence of a target gas. Target-gas densities $\lesssim 10^{11}$ $cm^{-3}$ are employed to ensure single-collision conditions. Rate constants $k_d$ for Rydberg-atom destruction in collisions are determined by measuring the time evolution of the Rydberg-atom population $N(t)$ in the interaction region. $N(t)$ is given to a good approximation by

$$N(t) = N(0)e^{-t/\tau}, \tag{3}$$

where

$$\frac{1}{\tau} = \rho k_d + \frac{1}{\tau_{\text{eff}}} \tag{4}$$

$N(0)$ is the number of Rydberg atoms present at $t = 0$ (i.e., at the end of the laser excitation pulse), $\tau_{\text{eff}}$ is the effective Rydberg-atom lifetime in the absence of the target gas, and $\rho$ is the target-gas density (measured by an ionization gauge calibrated against a capacitance manometer). In practice, the probability that a Rydberg atom is created during any laser pulse is small ($\lesssim 0.01$) and the time evolution of the population is obtained by applying a field ionizing pulse at a variable delay after each laser

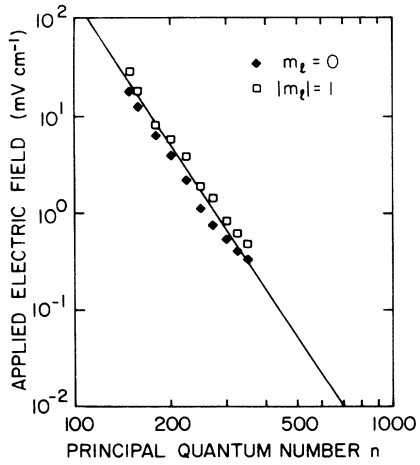


FIG. 4. Applied external electric field required to reduce the $np$ excitation efficiency by one-half. The solid line shows, for each value of $n$, the electric field at which states from adjacent hydrogenic Stark manifolds first cross.

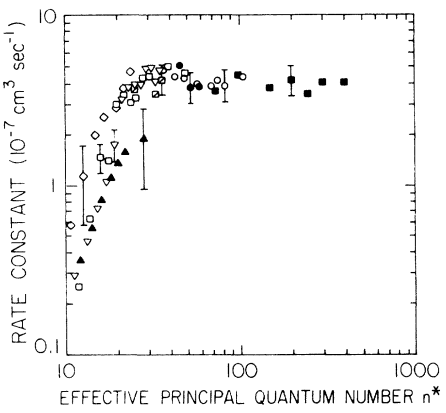


FIG. 5. Rate constants for Rydberg-atom destruction ($k_d$) and for free-ion production ($k_i$) in Rydberg atom collisions with $SF_6$. ■, $k_d$-K($np$) (present data); ○, $k_d$-Rb($nd$) (Ref. [2]); ●, $k_i$-Rb($ns$) (Ref. [2]); ⧄, $k_i$-Xe($nf$) (Ref. [1]); □, $k_i$-K($nd$) (Ref. [1]); ▽, $k_i$-Na($np$) (Ref. [16]); ◇, $k_i$-Ne($ns$) (Ref. [15]); ▲, $k_i$-Ne($nd$) (Ref. [15]).

pulse and accumulating data following many laser pulses. Values of $1/\tau$ are measured at several different target-gas densities $\rho$, and $k_d$ is obtained from a fit to the data using Eq. (4).

The measured rate constants $k_d$ for Rydberg-atom destruction in collisions with $SF_6$ and $CCl_4$ are shown in Figs. 5 and 6, respectively, as a function of effective principal quantum number $n^*$, where $n^* \equiv n - \delta$ and $\delta$ is the quantum defect. It has been demonstrated previously that for nonpolar attaching targets such as $SF_6$ and $CCl_4$, Rydberg-atom destruction results from Rydberg-electron capture and that, at high $n$, the rate constants $k_d$ for Rydberg-atom destruction can be equated to the rate constants $k_i$ for the production [1,2] of unbound $K^+$-$SF_6^-$ and $K^+$-$Cl^-$ ion pairs via reactions (1) and (2), respectively. This implies that the rate constants for collisional destruction through direct collisional ionization, i.e., through the reactions

$$K(np)+SF_6(CCl_4)\rightarrow K^+ + SF_6(CCl_4)+e^- , \quad (5)$$

are negligible in comparison to those for destruction through reactions (1) and (2). To check this, measurements of Rydberg-atom destruction were undertaken at $n \sim 250$ using $CO_2$ as the target gas. (Electron-$CO_2$ scattering is characterized by an unusually large momentum-transfer cross section at low energies [13].) The data showed that rate constants for Rydberg-atom destruction through direct collisional ionization are small and provided an upper limit for $CO_2$ (at $n \sim 250$) of $10^{-8}$ cm$^3$ sec$^{-1}$. Theory, however, suggests that rate constant for direct collisional ionization are typically substantially smaller than even this value [14]. Figures 5 and 6 include rate constants for collisional destruction and for the production of free ions measured by earlier workers [1,2,15,16]. Good agreement between the present data and the earlier measurements is observed. At low-to-intermediate values of $n$ the rate constants for the production of free ions decrease due to the increasing electrostatic attraction between the product positive and negative ions and the increasing opacity of the Rydberg-electron cloud. Both of these effects are discussed in detail elsewhere [17–20]. At high $n$, however, these effects are negligible and the free-electron model asserts that the rate constant for collisional destruction (and free-ion production) via reactions (1) and (2) should equal that for capture, by the target, of free electrons having the same velocity distribution as the Rydberg electron, i.e.,

$$k_d = \int_0^\infty v\sigma_e(v)f(v)dv , \quad (6)$$

where $f(v)$ is the Rydberg-electron velocity distribution (determined by its quantum state) and $\sigma_e(v)$ is the cross section for the capture of *free* electrons of velocity $v$. (Even at $n=400$ the root-mean-square orbital velocity of the excited electron, $\sim 6\times 10^5$ cm sec$^{-1}$, is much greater than the relative heavy-particle collision velocity, $\sim 6\times 10^4$ cm sec$^{-1}$.) It is apparent from Figs. 5 and 6 that for both $SF_6$ and $CCl_4$, the rate constants measured at very high $n$ are essentially independent of $n$, i.e., independent of the Rydberg-electron velocity distribution. Inspection of Eq. (6) shows that this independence requires that the attachment cross section be inversely proportional to electron velocity, i.e., inversely proportional to the square root of the electron energy $\varepsilon$. This behavior, $\sigma_e(\varepsilon) \propto \varepsilon^{-1/2}$, is consistent with the Wigner threshold law for $s$-wave attachment [21,22]. Analysis of the data shows that, if $v$ is expressed in cm sec$^{-1}$, $\sigma_e(v)$ is given by $(4.0\pm 1.0)\times 10^{-7}/v$ and $(8.5\pm 2.0)\times 10^{-7}/v$ cm$^2$ for $SF_6$ and $CCl_4$, respectively, for electron energies $\leq 2$ meV. To facilitate comparison with data for attachment of free electrons, velocity-averaged cross sections $\bar{\sigma}_e$ are derived from the Rydberg-atom data by use of the relation $\bar{\sigma}_e = k_{d,i}/v_m$, where $v_m$ is the median velocity of the electrons attached, i..e, the Rydberg-electron velocity, such that integration of Eq. (6) from 0 to $v_m$ yields a value one-half that for integration from 0 to $\infty$.

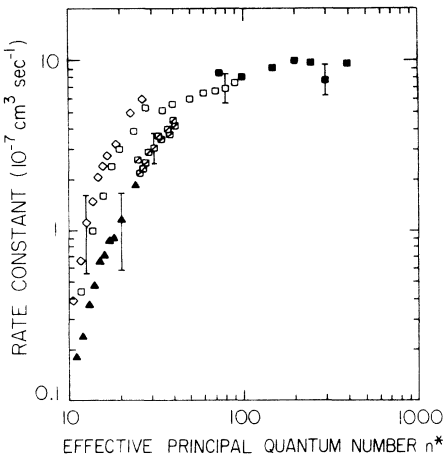


FIG. 6. Rate constants for Rydberg-atom destruction ($k_d$) and for free-ion production ($k_i$) in Rydberg atom collisions with $CCl_4$. ■, $k_d$-K($np$) (present data); □, $k_i$-K($nd$) (Ref. [1]); ⧄, $k_i$-Xe($nf$) (Ref. [1]); ◇, $k_i$-Ne($ns$) (Ref. [15]); ▲, $k_i$-Ne($nd$) (Ref. [15]).

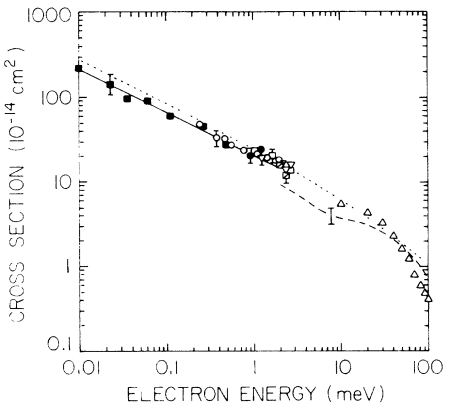


FIG. 7. Cross section for electron attachment to $SF_6$. ■, $\bar{\sigma}_e$-K($np$) present data; □, $\bar{\sigma}_e$-K($nd$) (Ref. [1]); ●, $\bar{\sigma}_e$-Rb($ns$) (Ref. [2]); ○, $\bar{\sigma}_e$-Rb($nd$) (Ref. [2]); , $\bar{\sigma}_e$-Xe($nf$) (Ref. [1]); △, swarm-unfold data (Ref. [23]); — — —, TPSA results (Ref. [22]); - - -, Klots (Ref. [26]); ——, $\sigma_e(v)$.

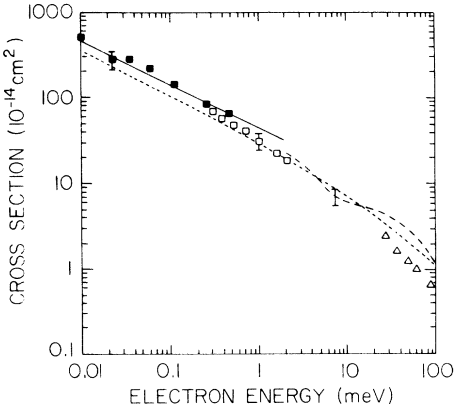


FIG. 8. Cross section for electron attachment to $CCl_4$. ■, $\bar{\sigma}_e$-K($np$) present data; □, $\bar{\sigma}_e$-K($nd$) (Ref. [1]); △, swarm-unfold data (Ref. [24]); — — —, TPSA results (Refs. [22,25]); - - -, Klots (Ref. [26]); ——, $\sigma_e(v)$.

The velocity-averaged cross sections $\bar{\sigma}_e$ are shown in Figs. 7 and 8 together with the corresponding cross sections $\sigma_e(v)$. The values of $\bar{\sigma}_e$ are positioned on the electron-energy axis according to the value of $mv_m^2/2$. Figures 7 and 8 also include data for free-electron attachment obtained using both swarm-unfold [23,24] and threshold photoelectron spectroscopy (TPSA) techniques [22,25], together with cross sections for electron capture derived using the theoretical expression for $s$-wave capture given by Klots [26], and polarizabilities of 6.52 and 10.6 Å$^3$ for $SF_6$ and $CCl_4$, respectively [27,28]. The agreement among the various data is good.

The present work shows that Rydberg-atom techniques can be used to measure cross sections for electron attachment and examine threshold behavior at ultralow electron energies, $\lesssim 10$ $\mu$eV, which are inaccessible using any alternate approach. The data confirm unequivocally that low-energy electron capture by $SF_6$ and $CCl_4$ is an $s$-wave process at threshold and demonstrate that Rydberg-atom collisions can be studied at very high $n$. Indeed, since application of the free-electron collision model is most easily justified at very large values of $n$, the study of Rydberg-atom collisions at very high $n$ promises to provide information on a wide variety of electron-molecule interactions at ultralow electron energies.

This research is supported by the National Science Foundation under Grant No. PHY8709637 and the Robert A. Welch Foundation.

[1] F. B. Dunning, J. Phys. Chem. **91**, 2244 (1987).
[2] B. G. Zollars, C. Higgs, F. Lu, C. W. Walter, L. G. Gray, K. A. Smith, F. B. Dunning, and R. F. Stebbings, Phys. Rev. A **32**, 3330 (1985).
[3] R. W. Marawar, C. W. Walter, K. A. Smith, and F. B. Dunning, J. Chem. Phys. **88**, 176 (1988).
[4] C. W. Walter, B. G. Lindsay, K. A. Smith, and F. B. Dunning, Chem. Phys. Lett. **154**, 409 (1989).
[5] C. W. Walter, K. A. Smith, and F. B. Dunning, J. Chem. Phys. **90**, 1652 (1989).
[6] A. Kalamarides, R. W. Marawar, M. A. Durham, B. G. Lindsay, K. A. Smith, and F. B. Dunning, J. Chem. Phys. **93**, 4043 (1990).
[7] For a discussion of the free-electron model see the articles by M. Matsuzawa and by A. P. Hickman, R. E. Olson, and J. Pascale in *Rydberg States of Atoms and Molecules,* edited by R. F. Stebbings and F. B. Dunning (Cambridge University Press, New York, 1983).
[8] B. G. Lindsay, K. A. Smith, and F. B. Dunning, Rev. Sci. Instrum. **62**, 1656 (1991).
[9] T. H. Jeys, G. B. McMillian, K. A. Smith, F. B. Dunning, and R. F. Stebbings, Phys. Rev. A **26**, 335 (1982).
[10] G. B. McMillian, T. H. Jeys, K. A. Smith, F. B. Dunning, and R. F. Stebbings, J. Phys. B **15**, 2131 (1982).
[11] M. L. Zimmerman, M. G. Littman, M. M. Kash, and D. Kleppner, Phys. Rev. A **20**, 2251 (1979).
[12] D. A. Harmin, Phys. Rev. A **30**, 2413 (1984).
[13] N. F. Lane, Rev. Mod. Phys. **52**, 29 (1980).
[14] V. S. Lebedev, J. Phys. B **24**, 1977 (1991); **24**, 1993 (1991).
[15] K. Harth, M. W. Ruf, and H. Hotop, Z. Phys. D **14**, 149 (1989).
[16] I. M. Beterov, G. L. Vasilenko, I. I. Riabstev, B. M. Smirnov, and N. V. Fateyev, Z. Phys. D **6**, 55 (1987).
[17] B. G. Zollars, C. W. Walter, F. Lu, C. B. Johnson, K. A. Smith, and F. B. Dunning, J. Chem. Phys. **84**, 5589 (1986).
[18] Z. Zheng, X. Ling, K. A. Smith, and F. B. Dunning, J. Chem. Phys. **92**, 285 (1990).
[19] X. Ling, M. A. Durham, A. Kalamarides, R. W. Marawar, B. G. Lindsay, K. A. Smith, and F. B. Dunning, J. Chem. Phys. **93**, 8669 (1990).
[20] A. Pesnelle, C. Ronge, M. Perdrix, and G. Watel, Phys. Rev. A **42**, 273 (1990).
[21] E. P. Wigner, Phys. Rev. **73**, 1002 (1948).
[22] A. Chutjian and S. H. Alajajian, Phys. Rev. A **31**, 2885

(1985).
[23] R. Y. Pai, L. G. Christophorou, and A. A. Christodoulides, J. Chem. Phys. **70**, 1169 (1979).
[24] A. A. Christodoulides and L. G. Christophorou, J. Chem. Phys. **54**, 4691 (1971).
[25] O. J. Orient, A. Chutjian, R. W. Crompton, and B. Cheung, Phys. Rev. A **39**, 4494 (1989).
[26] C. E. Klots, Chem. Phys. Lett. **38**, 61 (1976).
[27] A. D. Buckingham and R. E. Raab, J. Chem. Soc. **23**, 5511 (1961).
[28] A. Yoshihara, A. Anderson, R. A. Aziz, and C. C. Lin, Chem. Phys. **51**, 141 (1980).